

FLOW PATTERN NEAR MASSIF A IN THE YAMATO BARE ICE FIELD ESTIMATED FROM THE STRUCTURES AND THE MECHANICAL PROPERTIES OF A SHALLOW ICE CORE

Nobuhiko AZUMA¹, Masayoshi NAKAWO¹, Akira HIGASHI^{1*}
and Fumihiko NISHIO²

¹*Department of Applied Physics, Faculty of Engineering, Hokkaido University,
Kita-13, Nishi-8, Kita-ku, Sapporo 060*

²*National Institute of Polar Research, 9-10, Kaga 1-chome, Itabashi-ku, Tokyo 173*

Abstract: A shallow ice core, 30 m long, was collected at the Yamato bare ice field in East Queen Maud Land, Antarctica. From the uniaxial compression tests with the core, the flow law of the ice was obtained, which was different considerably from that obtained for the artificial polycrystalline ice with the random orientation fabric. Additional structural analyses (fabric, stratigraphy, etc.) of the core allowed estimation of the stress configuration and the flow field around the nunataks. As a result, a longitudinal stress of 0.15 MPa was obtained at the drilling site. Also, the variation of surface velocities, internal flow lines and isochrones upstream of Massif A were calculated. The results showed that the origin of the ice emerging near the nunataks is not far from its present position and the catchment area is rather small. The ice is considered nearly stagnant in the adjacent region of the nunataks.

1. Introduction

In East Queen Maud Land, flow of the ice sheet is partly obstructed by a chain of mountains lying along the edge of the continent. In order to clarify the influence of the presence of mountains on the stability of the ice sheet, it is important to study the dynamical behavior of the ice sheet near the mountains. For the development of a numerical model, the longitudinal stress which is considered to increase near mountains has to be taken into account. It is required, therefore, to assess the magnitude of the longitudinal stress based upon observations in the field.

NARUSE and HASHIMOTO (1982), and WHILLANS and CASSIDY (1983) calculated the internal flow lines of an ice sheet in the upstream area of the Yamato Mountains and the Allan Hills, respectively. Their calculations were performed on the basis of the continuity equation with some unrealistic assumptions, and no estimates were given on the longitudinal stress near the mountains. For the estimates, we have to know both the strain rate of the ice near a mountain and the flow law of the ice. The strain rate can be relatively easily obtained by field observations. The flow law to be used must be different from the generally accepted one obtained with artificial ice of random orientations of *c*-axes (BARNES *et al.*, 1971), because the fabric of ice near the mountains generally shows strong preferred orientations (NISHIO *et al.*, 1982). It

* Present address: Division of Natural Sciences, International Christian University, Mitaka-shi, Tokyo 181.

is necessary, therefore, to use a flow law obtained experimentally by the use of ice samples taken at the site in question.

In 1982, a 30 m long ice core was retrieved by a drilling performed by the 23rd Japanese Antarctic Research Expedition (JARE-23) upstream of Massif A in the Yamato bare ice field. In this paper, we tried to obtain a flow law for the core ice, based on mechanical tests of the core as well as its structural analysis. The surface flow line was also determined from the core analyses, which showed a trend that the ice flows down around the nunatak. Moreover, the internal flow lines and the iso-chrons near Massif A were calculated.

2. Flow Field at the Boring Site

The boring site (YM179) is shown in a partial relief map of the Yamato nunatak (Fig. 1). Suppose the origin at the surface of the boring site and the Cartesian coordinates are taken as shown in Fig. 2, the x -axis is on the horizontal plane, positive in the direction of flow, the y -axis is horizontal and perpendicular to the x -axis, and the z -axis is vertical, positive downward.

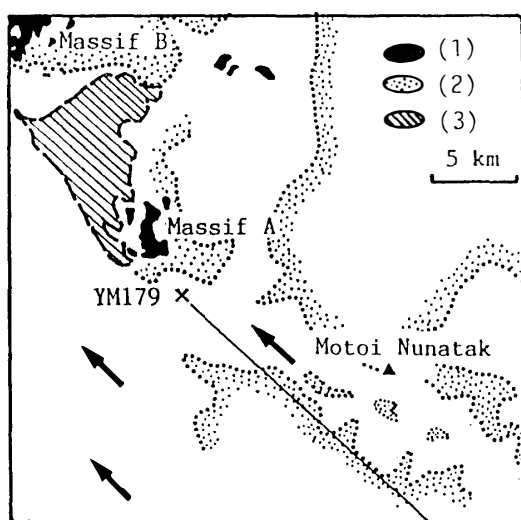


Fig. 1. The location of the boring site YM179. Arrows show the flow direction. (1) Nunatak, (2) snow-covered area, (3) moraine.

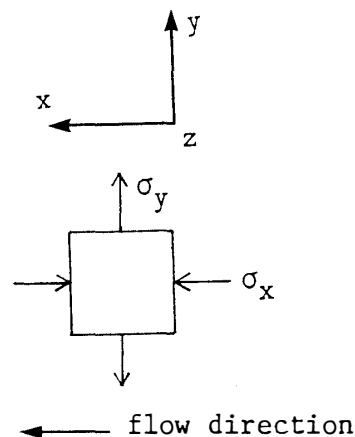


Fig. 2. Stress configuration at the boring site.

At the Yamato bare ice field, the ice tends to emerge out of the bottom and flows down around each nunatak, as the flow is dammed by the mountains. Downstream of the boring site, as shown in Fig. 1, there exist nunataks, which seem to hinder the ice flow through the site. Since many cracks are observed to run parallel to the flow direction, it would be reasonable to assume that the stress is compressive parallel to the direction of flow (x -axis), and tensile along y -axis. Surface cracks should open up in the direction of tensile stress, which can be one of three principal stresses (Nye, 1952). The three principal stresses, σ_1 , σ_2 , σ_3 , at the boring site, therefore, would

be equal to the following three normal stresses, σ_x , σ_y , σ_z , respectively, as shown in Fig. 2: σ_x and σ_z are compressive (negative sign), while σ_y is tensile (positive).

The normal strain rates can be expressed as:

$$\dot{\epsilon}_x = A_L \tau^{n-1} \sigma_x', \quad (1)$$

$$\dot{\epsilon}_y = A_T \tau^{n-1} \sigma_y', \quad (2)$$

$$n=3,$$

where

$$\tau = \frac{1}{\sqrt{6}} [(\sigma_y - \sigma_z)^2 + (\sigma_z - \sigma_x)^2 + (\sigma_x - \sigma_y)^2]^{\frac{1}{2}}, \quad (3)$$

and

$$\sigma_x' = \frac{1}{3} (2\sigma_x - \sigma_y - \sigma_z), \quad \sigma_y' = \frac{1}{3} (2\sigma_y - \sigma_z - \sigma_x). \quad (4)$$

Factors A_L and A_T are constants for a given temperature at the site. The values of A_L and A_T would be obtainable through uniaxial compression tests of ice samples with compression axis along x and y directions, respectively. With additional information on the values of σ_y , σ_z , $\dot{\epsilon}_x$ and $\dot{\epsilon}_y$, we can determine the longitudinal stress σ_x at the boring site.

The fabric diagrams of the YM179 ice core are shown in Fig. 3. The center of each diagram coincides with the vertical axis. Almost all fabric diagrams exhibit the great circle with a strong single maximum. The great circle plane of c -axes is nearly parallel to the planes of cracks in the ice core drawn by broken lines in the diagrams. The orientation of the single maximum of c -axes is parallel to the crack plane and inclined about 30° from the vertical. No cracks were found in the ice core below the depth of 20 m. Since the core was obtained without a mark for its orientation, when drilled, we estimated the flow direction as for the samples as follows: 1) The crack plane is parallel to the flow direction as observed in the field. 2) The strong concentration of c -axes would be inclined downglacier, since the ice would be the emergence flow toward a nunatak, being subjected mainly to the shear deformation on the basal plane of crystals. As for the diagram of 0.9 m deep in Fig. 3, for example, the flow direction was considered from right to left.

For obtaining the values of A_L and A_T , two kinds of specimens were prepared from the core. They would be subjected to the uniaxial compression along the directions parallel to the flow direction (x direction) as well as orthogonal to it (y direction) in a horizontal plane. For the latter test, from which we would obtain the value for A_T , a specimen of $20 \times 20 \times 60$ mm³ was cut out from a depth of 30 m with its long axis perpendicular to the great circle plane on the fabric diagram (specimen T). A preparation of a sample for the former test, *i.e.* with long axis parallel to the flow direction (specimen L), however, was not successful because of the limited size of the available core. Instead, a vertical specimen with the same size as specimen T was cut out from the core at the same depth (specimen V). By the uniaxial compression test with

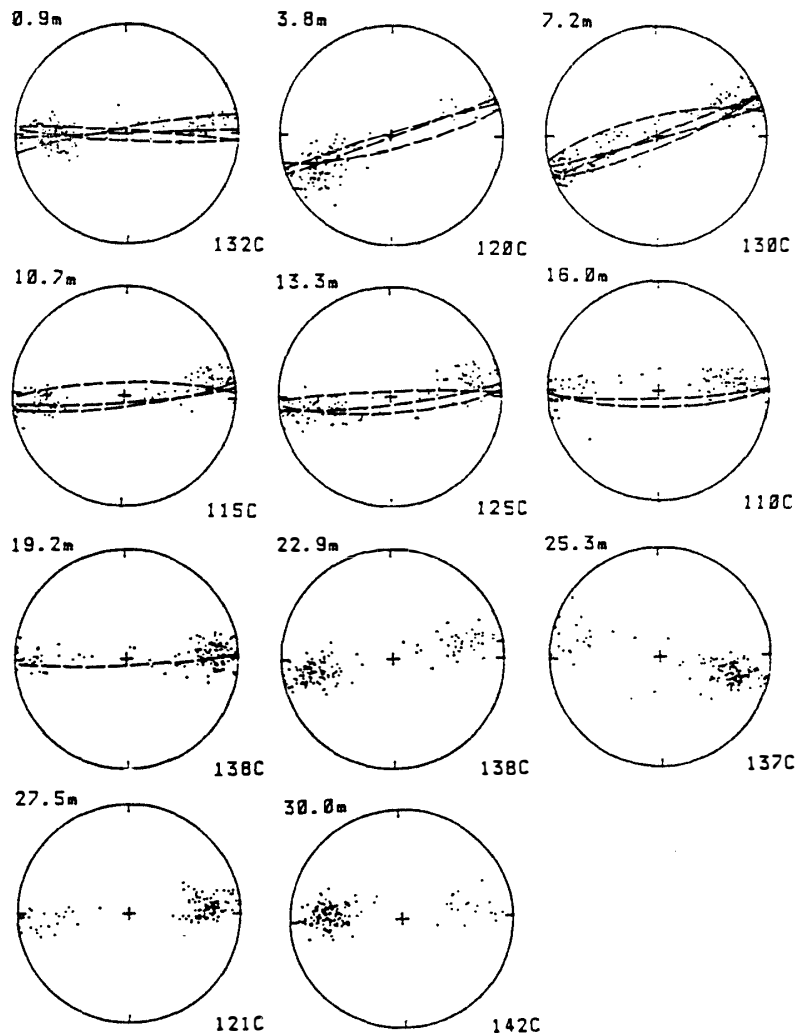


Fig. 3. Fabric diagrams for YM179 core. Center of the diagram coincides with the core axis. The number on the top left of each diagram indicates the depth in meters. The number of measured c -axes is shown on the bottom right.

this sample, a reasonable value for A_L would be obtainable because of the reasons mentioned below, although the compression axis is not parallel to the flow direction.

As can be seen in Fig. 3, the c -axes of crystals of the core were concentrated in orientation, forming a single maximum which inclined 60° from the horizontal plane and lay on the x - z plane. The ice would behave, hence, like a single crystal. Since a single crystal of ice easily glides on its basal plane, the deformation of the core ice would be attributed mainly to the shear deformation on the plane normal to the orientation of c -axis concentration. Let θ be the angle between the compression axis (flow direction) for specimen L and the preferred orientation of c -axes. For specimen V, on the other hand, the angle between the compressive axis (vertical direction) and the mean direction of c -axes is $\pi/2 - \theta$. Therefore, the relationships between the axial stress σ and the shear stress τ on the "mean basal plane" defined as the plane normal to the mean direction of c -axes are given by the following equations for specimens L and V, respectively:

$$\tau_L = \sigma \cos \theta \sin \theta,$$

$$\tau_V = \sigma \cos\left(\frac{\pi}{2} - \theta\right) \sin\left(\frac{\pi}{2} - \theta\right) = \sigma \cos \theta \sin \theta.$$

The suffix indicates the respective specimens of L or V. The relationships between the axial strain rate $\dot{\epsilon}$ and the shear strain rate $\dot{\gamma}$ on the “mean basal plane” are given by

$$\dot{\gamma}_L = \frac{\dot{\epsilon}}{\cos \theta \sin \theta},$$

$$\dot{\gamma}_V = \frac{\dot{\epsilon}}{\cos\left(\frac{\pi}{2} - \theta\right) \sin\left(\frac{\pi}{2} - \theta\right)} = \frac{\dot{\epsilon}}{\cos \theta \sin \theta},$$

and hence

$$\tau_L = \tau_V, \quad \dot{\gamma}_L = \dot{\gamma}_V.$$

Namely, a uniaxial test with a specimen V would be equivalent with a test using a specimen L.

Uniaxial compression tests with specimens T and V were carried out with a constant crosshead speed, which resulted in constant strain rate test: approximately $5 \times 10^{-7} \text{s}^{-1}$ for specimen V and approximately $5 \times 10^{-8} \text{s}^{-1}$ for specimen T. The uniaxial stress was measured by a wire strain gauge load cell attached to the crosshead of a test machine. The temperature in the vicinity of the specimen was monitored with a thermocouple, and kept at $-20.0 \pm 0.5^\circ \text{C}$ for specimen V and at $-10.0 \pm 0.5^\circ \text{C}$ for specimen T. When the crosshead started to move, the stress increased with increasing strain and finally reached a saturated value. In each test, when the stress reached a saturated value, the crosshead was stopped, and the specimen started to relax. We obtained the stress-strain rate relationships of the specimens from the relaxation curves. The details and the validity of this method will be published elsewhere.

The obtained relations are shown in Fig. 4, where dotted line indicates the results obtained by BARNES *et al.* (1971) for the artificial polycrystalline ice with the random orientation fabric. Their results as well as ours at -20°C and -10°C for specimens V and T respectively were all converted into the relationships at -30°C for comparison. From eqs. (1), (2), (3) and (4), the relationship between the axial strain rate $\dot{\epsilon}_x$ and the axial stress σ_x can be given by

$$\dot{\epsilon}_x = \frac{2}{9} A \sigma_x^3, \quad (5)$$

$$A = A_0 \exp\left(-\frac{Q}{KT}\right),$$

where A_0 is a constant, Q is the activation energy for creep ($60 \text{ kJ} \cdot \text{mol}^{-1}$, WEERTMAN, 1973), K is Boltzman constant and T is absolute temperature. From experimental results shown in Fig. 4 and eq. (5), we have thus obtained the value of A for each spec-

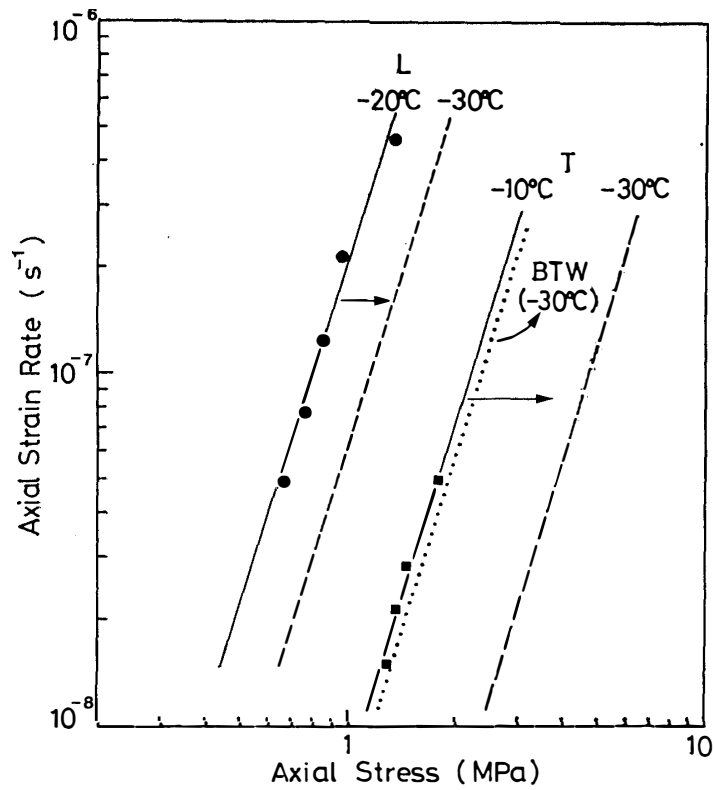


Fig. 4. Log-log plot of strain rate vs. stress relationship obtained from the mechanical tests. L: specimen L; T: specimen T; BTW: BARNES et al. (1971).

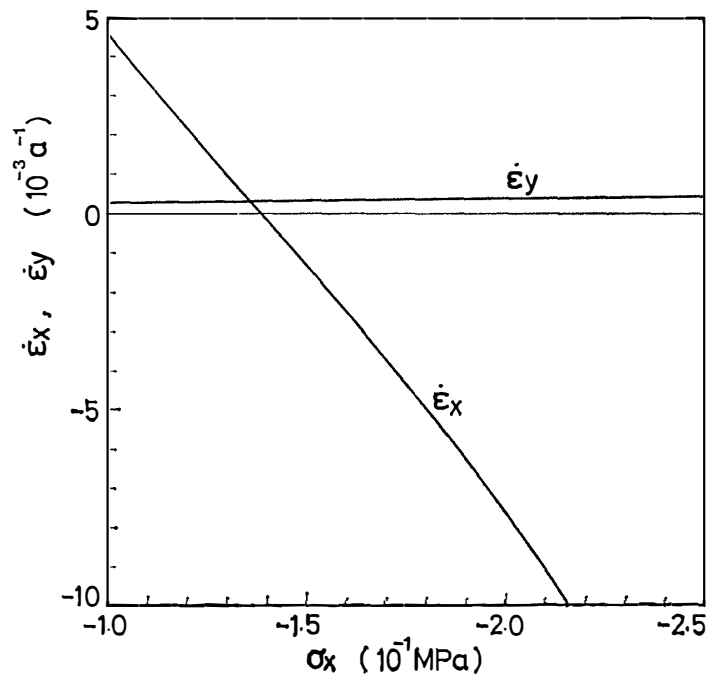


Fig. 5. Principal strain rates $\dot{\epsilon}_x$ and $\dot{\epsilon}_y$ vs. principal stress σ_x at the boring site.

imen at -30°C , which is the average temperature at the boring site: A_V is $2.8 \times 10^{-7} \text{ MPa}^{-3}\text{s}^{-1}$, which would be equivalent with A_L , and A_T is $3.6 \times 10^{-9} \text{ MPa}^{-3}\text{s}^{-1}$. They differ enormously from a value for the artificial polycrystalline ice ($3.8 \times 10^{-8} \text{ MPa}^{-3}\text{s}^{-1}$), presumably owing to the large difference in fabric.

Let us estimate the stresses at the boring site. Since cracks were closed at the depth of 20 m, we can consider the tensile stress σ_y normal to the crack plane would become zero at the depth. Three principal stresses would hence be given at $z=20$ m,

$$\sigma_x = ?, \sigma_y = 0, \sigma_z = -(P + \rho g z), \quad (6)$$

where P is atmospheric pressure, ρ is density of ice, and g is acceleration due to gravity. Substituting σ_y and σ_z from eq. (6) and the values of A_L and A_T into eqs. (1), (2), (3) and (4), we obtain relationships between strain rate $\dot{\epsilon}_x$ and $\dot{\epsilon}_y$ and stress σ_x at the boring site as shown in Fig. 5. The results indicate that $\dot{\epsilon}_x$ strongly depends on σ_x , while $\dot{\epsilon}_y$ is almost a constant of $3 \times 10^{-4} \text{ a}^{-1}$. No data are available on surface velocity and surface strain rate at the boring site, near Massif A, but the surface principal strain rate $\dot{\epsilon}_x$ of the order of 10^{-4} a^{-1} was measured by NARUSE (1978) at 2–3 km upstream from the Motoi Nunatak. Since the boring site is located also about 2 km upstream of Massif A, the strain rate $\dot{\epsilon}_x$ would be of the order of 10^{-4} a^{-1} at the boring site as well. The longitudinal stress σ_x can be estimated, then, being about 0.15 MPa from Fig. 5.

3. Surface Flow Line and Surface Velocity

Co-ordinate axis x is taken parallel to the flow direction but positive upstream, and z -axis vertical but positive upward this time. The axis y is taken, so as to become right-handed, perpendicular to the flow direction. The origin is taken on the sea level at the glacier snout in contact with Massif A in the Yamato Mountains (see Fig. 1).

The distance between the given two adjacent flow lines in the vicinity of x -axis would increase gradually with approach to the nunatak. It would be reasonable, therefore, to assume that the width, W can be given by the following exponential function of x

$$W = ae^{bx} + c, \quad (7)$$

and

$$b = -\frac{\ln a}{2000},$$

where a and c are constants. We would further assume that the width W to be independent on depth as a first approximation. The mass flux at x through a vertical cross section between two flow lines, as shown in Fig. 6, is expressed as

$$Q = WH\bar{u}, \quad (8)$$

where H is ice thickness and \bar{u} is the x component of mean ice velocity through the vertical cross section at x . They are given by

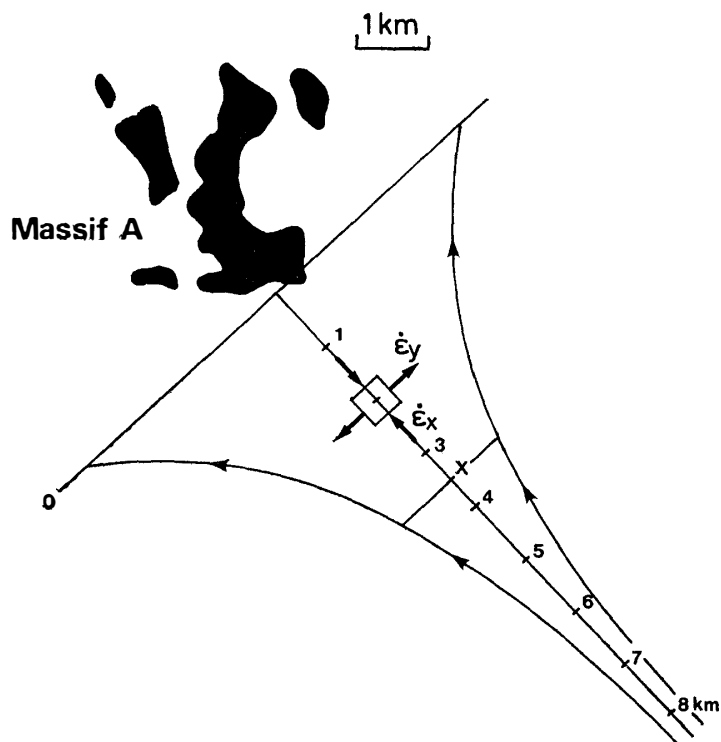


Fig. 6. Surface flow line near Massif A.

$$H = Z_s - Z_B, \quad (9)$$

$$\bar{u} = \frac{1}{H} \int_{z_B}^{z_s} u(z) dz, \quad (10)$$

where Z_s and Z_B are the surface elevation of the ice sheet and the bed rock elevation, respectively. On the basis of the data obtained from the Data Compilation of "Nankyoku no Kagaku" (KOKURITSU KYOKUCHI KENKYUJO, 1985), Z_s and Z_B are approximated by

$$Z_s = 0.179x^{0.716} + 2140 \text{ (m)}, \quad (11)$$

and

$$Z_B = 1140e^{-3.3 \times 10^{-5}x} + 1000 \text{ (m)}, \quad (12)$$

at various distances from the snout. Assuming the flow is laminar, the x component of the ice velocity at a given depth z is expressed by

$$u(z) = u_s \left(1 - \left(\frac{z_s - z}{H} \right)^{n+1} \right), \quad (13)$$

where u_s is the x component of the surface velocity, and n is a constant which we assume being 3. Substitution of eqs. (9) and (13) into eq. (10) gives

$$\bar{u} = M u_s, \quad (14)$$

where

$$M=4/5 \text{ for } n=3.$$

Surface velocity u_s is assumed zero at the snout ($x=0$). With the steady state condition the mass flux through the vertical cross section has to be equivalent with the mass balance at the surface. Hence,

$$Q = \int_0^x BW \, dx, \quad (15)$$

where B is the surface balance assumed to be independent on time and given by

$$B = -0.05 \text{ m/a} \quad (0 \leq x < 30 \text{ km}),$$

$$B = 0.015x - 0.5 \text{ m/a} \quad (30 \leq x < 40 \text{ km}),$$

$$B = 0.1 \text{ m/a} \quad (x \geq 40 \text{ km}),$$

which are based upon the data by YAMADA *et al.* (1978). From eqs. (8), (14) and (15)

$$u_s = \frac{5}{4WH} \int_0^x BW \, dx. \quad (16)$$

When the width W is known, *i.e.*, the values of a and c are given (eq. (7)), the x component of the surface velocity, u_s , can be obtained for a given x . The surface strain rate $\dot{\epsilon}_{xs}$ and $\dot{\epsilon}_{ys}$ also can be obtained by the following equations:

$$\dot{\epsilon}_{xs} = \frac{\partial u_s}{\partial x}, \quad (17)$$

$$\dot{\epsilon}_{ys} = \frac{u_s}{W} \frac{\partial W}{\partial x}. \quad (18)$$

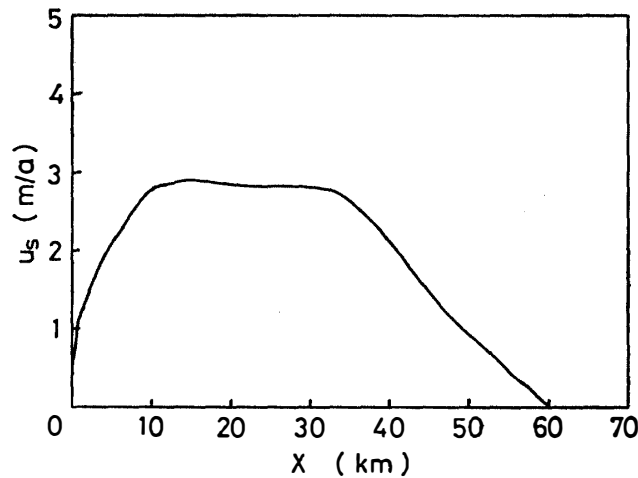


Fig. 7. Calculated results of the horizontal component of surface velocity upstream of Massif A.

We selected the values of a and c , therefore, so that the calculated values of $\dot{\epsilon}_{xs}$ and $\dot{\epsilon}_{ys}$ at the boring site ($x=2000$ m) become of the order of $-10^{-4}a^{-1}$ and $3 \times 10^{-4}a^{-1}$, respectively, as described in the previous section. The values of about 1.8 and 0.4 were thus obtained for a and c , respectively. The x component of surface velocity, u_s , calculated from eq. (16) with the values of a and c are shown in Fig. 7.

4. Internal Flow Lines and Isochrones

Using the surface velocity and the surface strain rate obtained in the previous section, we estimated the internal flow lines and isochrones of ice upstream of the nunatak. Since the x component of ice velocity, u , at a given position (x, z) is expressed by eq. (13), we can calculate the period Δt which is the time required to travel for a short distance Δx at the position.

The mean vertical strain rate $\bar{\epsilon}_z$ from the surface to the bedrock at x may be written as follows (WHILLANS, 1977):

$$\bar{\epsilon}_z = M \dot{\epsilon}_{zs}, \quad (19)$$

where,

$$M = \frac{4}{5} \text{ for } n=3,$$

and

$$\dot{\epsilon}_{zs} = -(\dot{\epsilon}_{xs} + \dot{\epsilon}_{ys}). \quad (20)$$

The vertical travel distance Δz is, hence, given by

$$\Delta z = \bar{\epsilon}_z \cdot \Delta t \cdot (z - z_B). \quad (21)$$

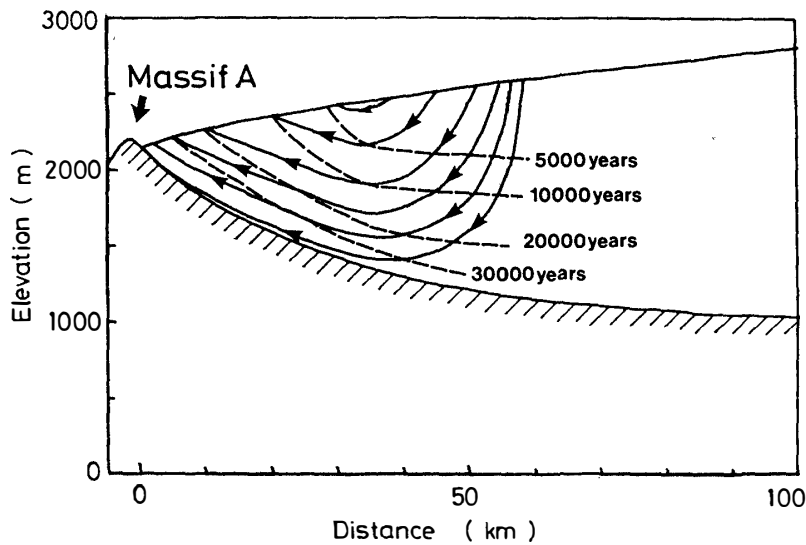


Fig. 8. Internal flow line and isochrones upstream of Massif A.

By using the values of $\dot{\epsilon}_{xs}$, $\dot{\epsilon}_{ys}$ and u_s obtained in the previous section, the vertical travel distance Δz was estimated for Δx . The calculations were made with a 100 m interval, *i.e.* $\Delta x=100$ m. The particle trajectories and isochrones for ice upstream of the nunatak were thus obtained as shown in Fig. 8. The results indicate that the ice found in the vicinity of the nunatak is originated at around 60 km upstream of the nunatak in an extreme case, and the age of the ice is about several tens thousand years.

5. Concluding Remarks

A longitudinal stress at the boring site was estimated at 0.15 MPa and the surface flow line in the vicinity of the nunataks was determined from the analyses of the structures and the mechanical properties of the shallow ice core. A flow model developed in this paper revealed that the origin of the ice emerging in the Yamato bare ice field is not far from the nunataks and its catchment area is rather small. In the model, however, the ice sheet was assumed to be in a steady state. Further we used the laminar flow approximation in which the longitudinal stress is not taken into account. In order to develop more realistic models, it is desirable to know the horizontal and the vertical distribution of the longitudinal stress in a wide region upstream of a nunatak from the structural studies and the mechanical tests of the multiple ice cores in the bare ice field.

References

- BARNES, P., TABOR, D. and WALKER, J.C.F. (1971): The friction and creep of polycrystalline ice. *Proc. R. Soc. London, Ser. A*, **324**, 127–155.
- KOKURITSU KYOKUCHI KENKYŪJO, ed. (1985): *Nankyoku no Kagaku 9. Shiryō-hen* (Science in Antarctica, 9. Data Compilation), Tokyo, Kokon Shoin, 56–57.
- NARUSE, R. (1978): Surface flow and strain of the ice sheet measured by a triangulation chain in Mizuho Plateau. *Mem. Natl Inst. Polar Res., Spec. Issue*, **7**, 198–226.
- NARUSE, R. and HASHIMOTO, M. (1982): Internal flow line in the ice sheet upstream of the Yamato Mountains, East Antarctica. *Mem. Natl Inst. Polar Res., Spec. Issue*, **24**, 201–203.
- NISHIO, F., AZUMA, N., HIGASHI, A. and ANNEXSTAD, J. O. (1982): Structural studies of bare ice near the Allan Hills, Victoria Land, Antarctica; A mechanism of meteorite concentration. *Ann. Glaciol.*, **3**, 222–226.
- NYE, J. F. (1952): The mechanics of glacier flow. *J. Glaciol.*, **2** (12), 82–93.
- WEERTMAN, J. (1973): Creep of ice. *Physics and Chemistry of Ice*, ed. by E. WHALLEY *et al.* Ottawa, Royal Society of Canada, 320–337.
- WHILLANS, I. M. (1977): The equation of continuity and its application to the ice sheet near “Byrd” Station, Antarctica. *J. Glaciol.*, **18** (80), 359–371.
- WHILLANS, I. M. and CASSIDY, W. A. (1983): Catch a falling star; Meteorites and old ice. *Science*, **222**, 55–57.
- YAMADA, T., OKUHIRA, F., YOKOYAMA, K. and WATANABE, O. (1978): Distribution of accumulation measured by the snow stake method in Mizuho Plateau. *Mem. Natl Inst. Polar Res., Spec. Issue*, **7**, 125–139.

(Received June 24, 1985; Revised manuscript received August 29, 1985)